SHAPE RESPONSE OF PLEISTOCENE AND RECENT SEDIMENT--CHUKCHI SEA: A FOURIER ANALYSIS

Thesis for the Degree of M. S.
MICHIGAN STATE UNIVERSITY
JAMES WATON KENNEDY
1972

ABSTRACT

SHAPE RESPONSE OF PLEISTOCENE AND RECENT SEDIMENT--CHUKCHI SEA: A FOURIER ANALYSIS

By

James Waton Kennedy

A Fourier analysis of grain shape was performed to determine if sand grain shape is a variable which will display some general utility in making inference about provenance, transport and depositional environment of Holocene sediments in the Chukchi Sea.

The shape, expressed as amplitudes of a Fourier series, was analyzed using both a pattern recognition-clustering program, ISODATA, and a complex analysis of chi-square contingency tables.

The results indicate that the shape variable is extremely sensitive to changes in provenance, transport and depositional environment.

SHAPE RESPONSE OF PLEISTOCENE AND RECENT SEDIMENT--
CHUKCHI SEA: A FOURIER ANALYSIS

By

James Waton Kennedy

A THESIS

Submitted to
Michigan State University
in partial fulfillment of the requirements
for the degree of

MASTER OF SCIENCE

Department of Geology

1972

675691

ACKNOWLEDGMENTS

I gratefully acknowledge Dr. Joe S. Creager, of the University of Washington Department of Oceanography, and National Science Foundation Grant GA 28002, for providing me with the samples on which this research was based. Dr. Creager's comments, criticisms and suggestions were invaluable to the success of this project.

I also extend grateful appreciation to Dr. Robert Ehrlich, my thesis advisor, for his tireless effort and enthusiasm throughout the entire project. Without his constant encouragement and helpful discussions this project would have taken considerably more time.

Dr. Bernhard Weinberg, of the Computer Science Department at Michigan State was extremely helpful in working out and assisting in many of the computer programs used.

Thanks also go to Drs. Sam Upchurch and Robert Anstey, my committee members, whose criticisms were quite helpful.

Last, but not least, I wish to express my sincere gratitude to my wife, Sharon, for her patience and understanding throughout the entire period, during which the project often took precedence over the family.

TABLE OF CONTENTS

LIST OF TABLES

LIST OF FIGURES

CHAPTER I

INTRODUCTION

The Chukchi Sea is located to the north of the Bering Strait, between Alaska and Siberia (Figure 1). As shown by Creager and McManus et al. (1969), the surface dispersal mechanisms and characteristics are markedly influenced by the strong northward flowing Bering Strait Current, which introduces silts and sands from a Yukon River source to the south into the Chukchi Sea. During the last glacial maximum, sea level was lowered sufficiently to expose all of the Chukchi Sea south of Wrangel Island permitting a subaerial erosion surface to develop. As sea-level rose, a transgressive sedimentary sequence was deposited over this surface. Initially the sediment available for dispersal and inclusion in the transgressive sequence was the reworked surface sediment and detrital sediment from the surrounding land mass. The main sediment source was the Kobuk and Noatak rivers and their drainage basins (Creager and McManus, 1965). This sedimentary regime must have changed dramatically after the sill at Bering Strait was breached by rising sea level, permitting establishment of the Bering Strait Current and the introduction of its sediment load.

The significant change in sediment source should produce a marked change in sediment character within the transgressive sediment

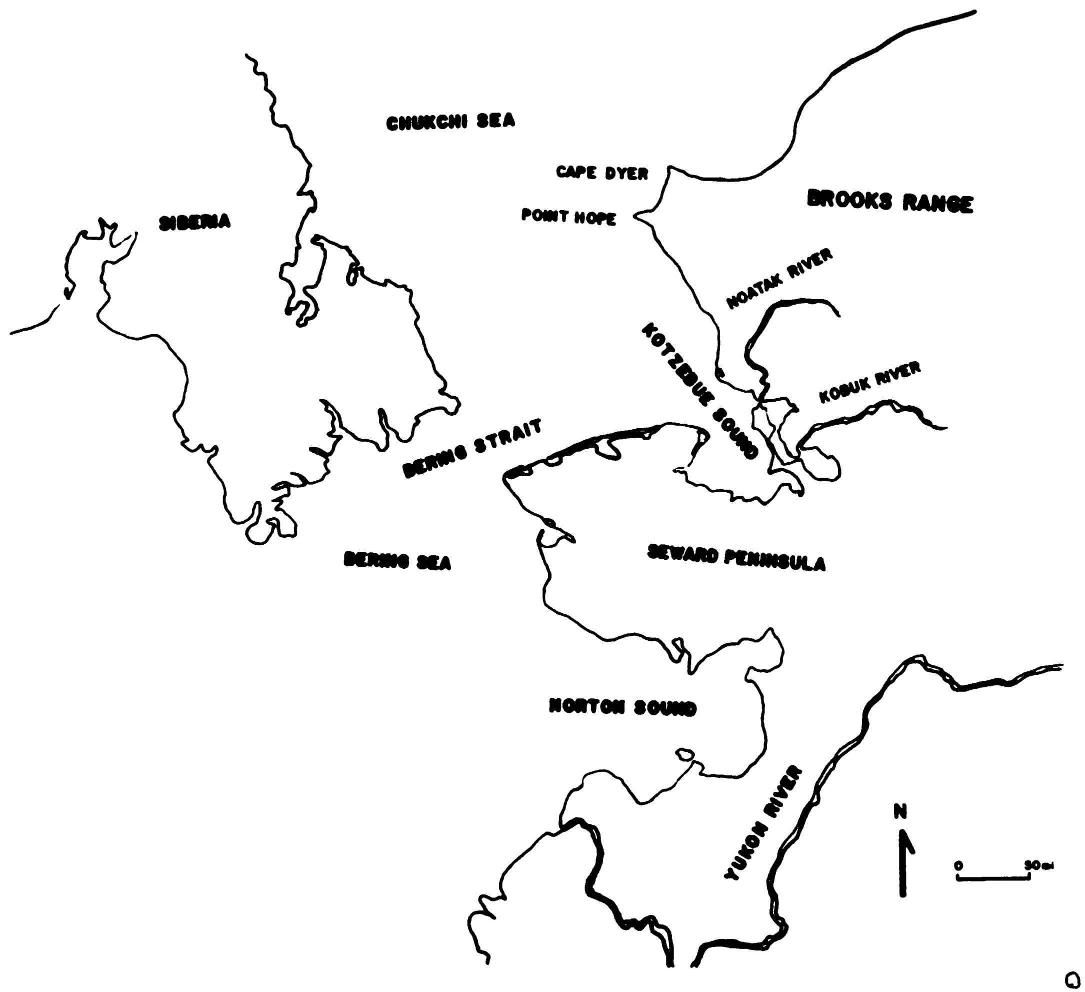

FIGURE 1.--General location map of Chukchi Sea region (after Creager).

sequence north of Bering Strait that identifies the time of introduction of first Yukon River sediment.

Ehrlich and Weinberg (1970), have shown that grain shape, if characterized exactly, can carry important information concerning both the provenance of sediments and their response to various processes.

Assuming this method is effective, then a powerful tool exists for objectively interpreting the sedimentary record in this area. It was toward this end then, that the Chukchi Sea samples were evaluated.

CHAPTER II

GENERAL STATEMENT OF PROBLEM

As part of a more comprehensive study of the Holocene history of the Chukchi Sea, a detailed stratigraphy of the last transgressive sedimentary sequence has been formulated (Creager et al., in preparation). On the basis of texture, mineralogy, microfauna, subbottom profiles, and radiocarbon dates, the type stratigraphy of the transgressive sequence north of the Bering Strait and west of Point Hope consists from the base upwards of a) Z-clay--a barren, compacted pre-Holocene sediment separated unconformably from an overlying; b) B-sand--a basal sand presumably deposited near sea-level along the shores of a large Kobuk-Noatak estuary; c) A' clay--an upward fining sediment deposited in gradually deepening water; d) A" silt overlain by A' silt--upward coarsening sediments postulated as resulting from introduction of silt from the south; e) A sand--a sand deposited under fairly stable sea-level conditions. Immediately north of Bering Strait the A sand is interpreted as part of a northward moving depositional front associated with Bering Strait Current. Elsewhere the A sand is believed to be reworked basal sand or of local derivation.

Clearly, sediment in the Chukchi Sea has been affected by a variety of provenance, transport and depositional effects. The sediment emanating from the Kobuk-Noatak and Yukon drainages have different provenances. In addition these sediments have undergone differing degrees of ice action (perma-frost, sea or glacial ice). During transport much of these sediments suffered transportation abrasion on beaches and in rivers. Sediments affected by some or all of these factors, some of which involve the opening of the Bering Strait, are now present in the Chukchi Sea.

Thus, if Fourier shape analysis results indicate a lack of significant difference between samples, this will tend to reflect more upon the adequacy of the method, rather than a high degree of homogeneity in the provenance and history of the samples.

Alternatively, the presence of significant differences between samples would permit useful interpretations relative to the depositional history postulated in the stratigraphic sequence presented above.

Significant differences do, in fact, exist. However, because of the small number of samples, a detailed explanation for these differences cannot now be undertaken.

Samples were collected to test hypotheses concerning past and present sedimentary provenance and transport hypotheses.

Bathymetry, Paleobathymetry and Currents

Comparison of the present bathymetry (Figure 2) with the paleobathymetry of the pre-Holocene transgression surface (Figure 3) clearly indicates the significance of the Bering Strait Current derived sediment in changing the bathymetry of the Chukchi Sea continental shelf surface north of Bering Strait. The paleobathymetric sill had depths of 50-52 meters but the modern sill is at depths of

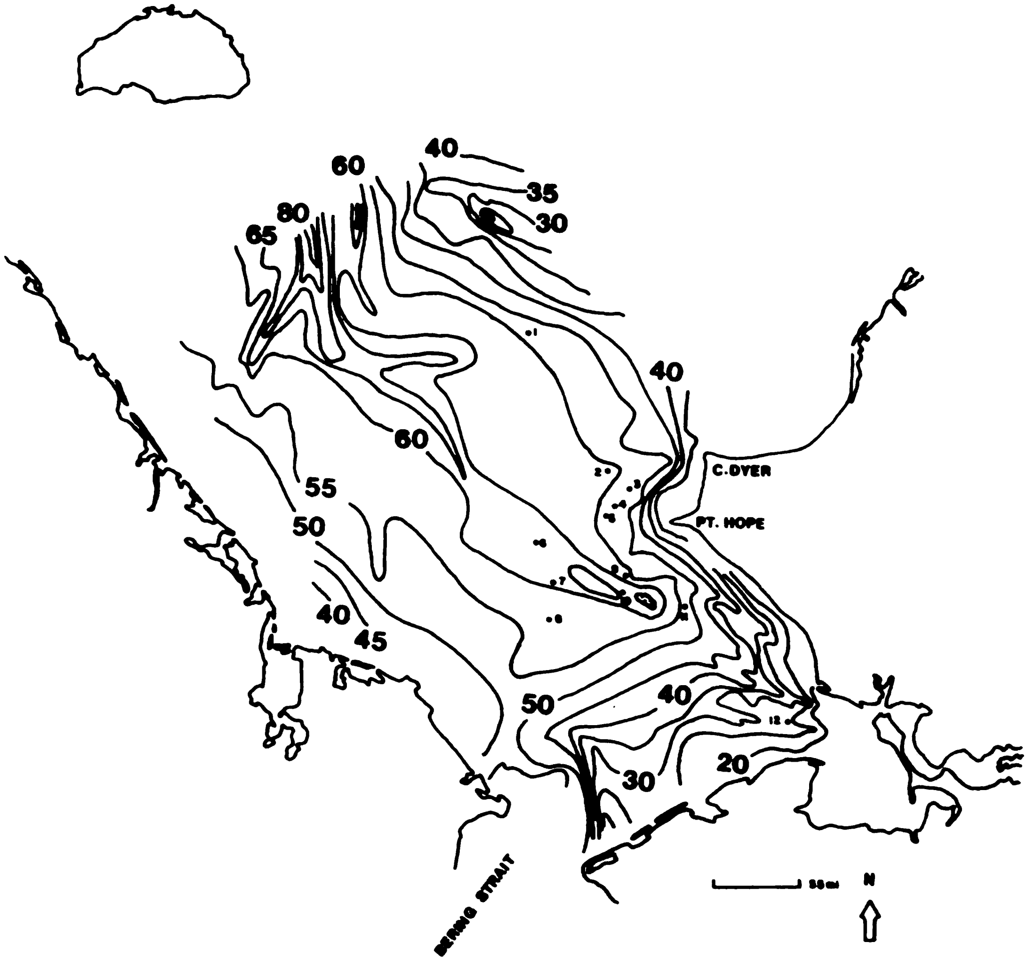

FIGURE 3.--Pre-B sand bathymetry of Chukchi Sea (contours in meters; after Creager).

46-48 meters. The filled valley south of Cape Thompson (Figures 2, 3) is related to a previous lower sea level--Kobuk-Noatak delta (Creager and McManus, 1967).

In deciphering the transgressive history of the Chukchi Sea sediments it is of permanent importance to: (1) specifically identiby, if possible, each sand unit as either a wave reworked shallow-water transgressive sand or a deeper-water current transported advancing depositional front sand; and (2) identify characteristics of a sediment which can place its source and hence identify the onset of sediment contribution by the Bering Strait Current (Figures 4 and 5). It is of interest, then, to examine two separate analytical hierarchies in the contingency tables, in order that both an overall A-B contrast and overall between A and between B comparisons can be made. Additionally, individual A-B comparisons and between-core contrasts are useful.

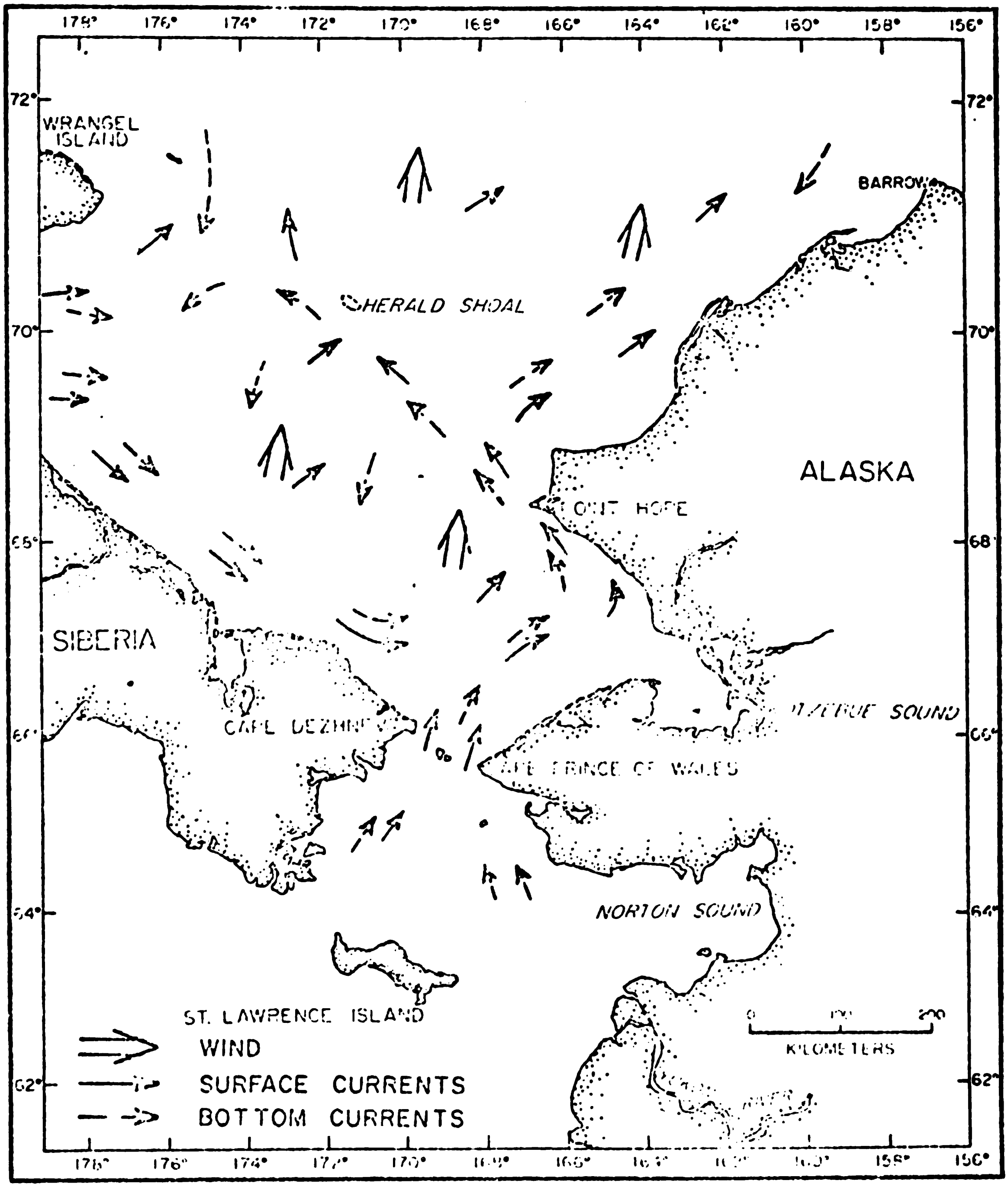

FIGURE 4.--Schematic current pattern with south wind (after Creager).

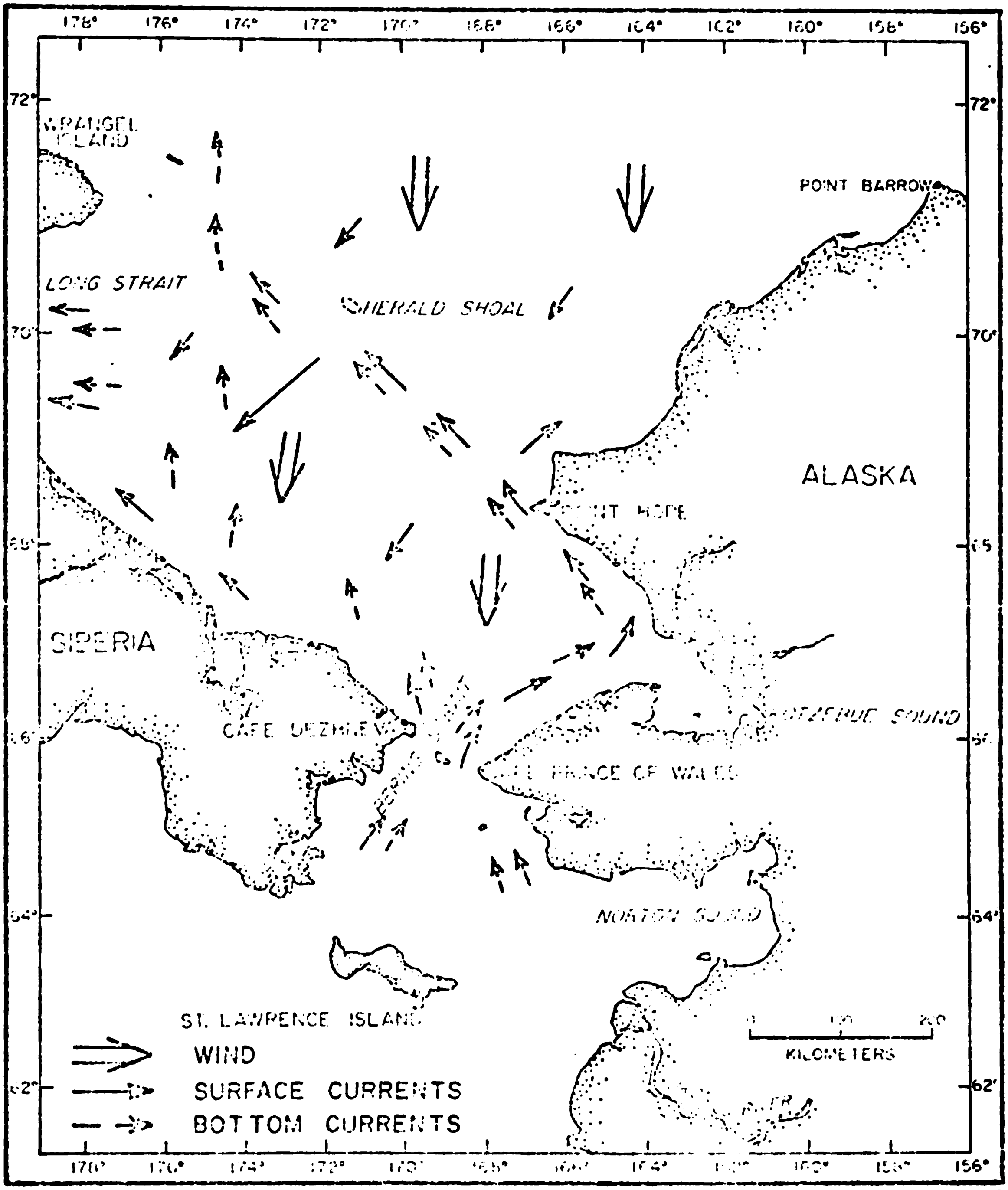

FIGURE 5.--Schematic current pattern with north wind (after Creager).

CHAPTER III

METHODS

In evaluating the grain shape of the Chukchi Sea samples, quartz was chosen as the mineral to be analyzed. The reason for choosing quartz, vis-a-vis some other mineral was two-fold. First of all, quartz is ubiquitous. Secondly, quartz shape, because of its presumed lack of cleavage control, was thought to carry a more uniform response history to the processes at work in eroding, transporting and ultimately depositing the sediment. The size of the grains analyzed ranged from medium silt to medium sand.

In preparing samples for analysis, they were first thoroughly washed, in order to remove most of the fine, organic rich muds holding the grains together. After filtering and drying, the grains were mounted on petrographic slides using a mounting oil. The grains, when strewn on the slide, would then theoretically position themselves in their area of maximum projection.

In order that the shape would be characterized as exactly as possible, a camera lucida was used which projected the image of the grain onto a starburst pattern, consisting of 48 radial lines of equal angular spacing, upon which the outline of the grain was traced. An automatic digitizer was then employed which would assign a four digit X, and a four digit Y co-ordinate to each point at which the grain boundary crossed one of the 48 radial lines, and punch these coordinates in a counterclockwise pattern onto Hollerith cards.

It has been shown empirically (Redmond, 1969; Waltz, 1972; Orzeck, 1972), that a sample size of 100 grains is sufficient to overcome any bias due to incorrect digitization of a small number of grains.

Once digitized, the first twenty harmonics of a Fourier series were calculated for each grain using a computer program developed by Dr. Bernhard Weinberg (see Ehrlich and Weinberg, 1970, for a discussion of Fourier analysis of grain shapes).

Each sample, consisting of 100 grains, the shape of each described by values of 19 harmonic amplitudes, was evaluated by a pattern recognition procedure, ISODATA. ISODATA is an acronym for Iterative Self Organizing Data Analysis Technique (A) (Ball and Hall, 1967). ISODATA is a clustering technique for multi-variate data which uses an average response pattern to represent a group of patterns. The endpoint of this technique is to minimize the sum of the squared distances of each data point from the nearest cluster center (Ball and Hall, 1967). The resulting output then, has distributed the grains in each sample into clusters, the mean shape of which can be inferred from an analysis of the harmonic amplitudes of the cluster centers.

In addition, a complex analysis of chi-square contingency tables was performed, harmonic by harmonic, using samples as rows, as the harmonic amplitude variation divided into six categories and the columns. The chi-square analyses were performed to identify those harmonics that carried significant shape information and to locate the origin of significant variation within each such harmonic. The degrees of freedom of the total chi-square was partitioned in a manner equivalent to Kimball's method for partitioning degrees of freedom in chi-square (Kimball, 1954).

The chi-square analyses were hierarchical in character. However, two different hierarchies were evaluated; one for harmonics 2-10, and another for harmonics 11-20.

The hierarchy employed for harmonics 2-10 included an overall test for A sands versus B sands, as well as breakdowns to show selected within and between A sand variations. For harmonics 11-20, the hierarchy was selected so as to test for significant variation between A and B sands within single cores, as well as to test for significant between-core variation.

Admittedly this procedure injects some ambiguity into data interpretation. However, all comparisons must, by definition, be established before data are inspected. In the case of the Chukchi Sea samples, two hierarchies were of equal interest. Both, however, could not be performed on the same set of data. Therefore, separate hierarchical analysis of harmonics 2-10, and 11-20 were performed.

This procedure depends on redundancy between the two sets of data, an assumption warranted by previous studies (Redmond, 1969; Waltz, 1972; Orzeck, 1972). Tables 1 and 2 show the hierarchies employed in the contingency tables. Table 3 shows how the members of the hierarchies are related to the core locations that are displayed on Figure 6.

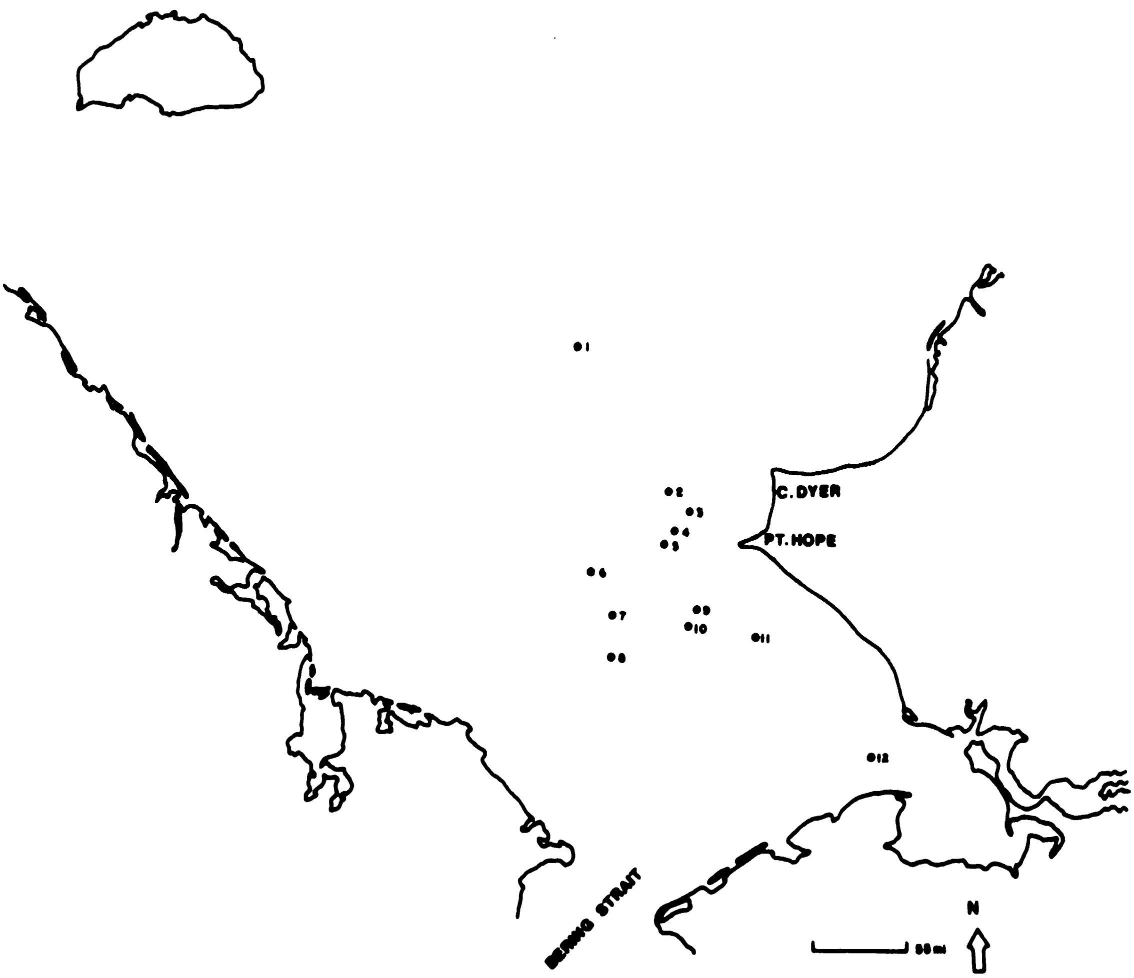

FIGURE 6.--Map showing core locations (see TABLE 3 for sample designations).

TABLE 1.--Results of contingency tables for hierarchy I.

Source of variability	d.f.	Harmonic 2	3	4	5	6	7	8	9	10
Total	85								X	X
A vs B*	5									
Within A vs B	80	X							X	X
Between A	35									X
$A_{2+3+4+5+9+12}$ vs A_1+A_8	5	X								
A_{1+8} vs A_2 vs 3vs4vs5 vs9vs12	30									X
A_1 vs A_8	5									X
Between $A_{2,3,4,5,9,12}$	25								X	X
A_{12} vs $A_{2+3+4+5+9}$	5									
Between $A_{2,3,5,9}$	20							X	X	X
A_9 vs $A_{2+3+4+5}$	5							X		
Between $A_{2,3,4,5}$	15								X	X
Between B	45									

X indicates significance at 5% level

* See TABLE 3 for explanation of A and B sand subscripts.

TABLE 2.--Results of contingency tables for hierarchy II.

Source of variability	d.f.	Harmonic 11	12	13	14	15	16	17	18	19	20
Total	80			X	X		X	X	X		
Between cores	25										X
Bet. A vs B W/cores	30			X							
A_1 vs B_1	5										
A_2 vs B_2	5	X	X	X	X	X		X	X		
A_3 vs B_3	5				X						
A_4 vs B_4	5										
A_5 vs B_5	5										
A_9 vs B_9	5										
Tot. bet. unpaired A and B	20						X	X	X		X
A_8 vs A_{12}	5						X				
B_7 vs B_{10} vs B_{11}	10		X						X		
A_8+A_{12} vs $B_7+B_{10}+B_{11}$	5			X	X		X	X	X		

X indicates significance at 5% level

* See TABLE 3 for explanation of A and B sand subscripts.

TABLE 3.--Sample designations as related to contingency table hierarchies, and sample locations.

Yukon vs Noatak-Kobuk Comparison				A Sand vs B Sand Comparison					
Sample	Core Location On Figure 6	Stratigraphic Unit Designation for this paper		Sample	Core Location On Figure 6	Stratigraphic Unit Designation for this paper			
						A Sand		B Sand	
TT51-4-014	(8)	A sand	(A_8)	TT20-16-19	(12)	X	(A_{12})		
TT20-39-109	(7)	A' silt		TT20-33-83	(5)	X	(A_5)	X	(B_5)
TT20-39-109		A" silt		TT20-34-87	(4)	X	(A_4)	X	(B_4)
TT20-39-109		A' clay		TT20-35-90	(2)	X	(A_2)	X	(B_2)
TT20-39-109		B sand		TT20-46-127	(9)	X	(A_9)	X	(B_9)
TT20-38-105	(6)	Z clay		TT20-50-137	(3)	X	(A_3)	X	(B_3)
				TT20-68-202	(1)	X	(A_1)	X	(B_1)
				TT51-02-7	(10)			X	(B_{10})
				SI689-62	(11)			X	(B_{11})

CHAPTER IV

RESULTS

The first hierarchy, evaluating harmonics 2-10, was designed to evaluate the Chukchi Sea samples from a stratigraphic point of view. This hierarchy tested for differences within and between stratigraphic units.

The second hierarchy, involving harmonics 11-20, was designed primarily to evaluate the differences between cores and within cores.

Hierarchy I

In the first hierarchy, the overall contrast between A and B sands was evaluated. If the A and B sands do, in fact, represent separate transport histories and depositional environments with no mixing of sediment, it would be expected that the results of this contrast should be statistically significant.

The results do, however, indicate no significant difference between A and B sands for any of the harmonics thus evaluated.

These results indicate either that the A and B sands are, in fact, everywhere homogeneous, or that they change in character from core to core in an irregular manner. For reasons which will become clearer upon looking at the second hierarchy, the latter explanation is favored.

Orthogonal comparisons at lower levels of hierarchy I evaluate the significance of differences between samples of A sand that differ in location

Because there was little "a priori" reason, such a breakdown was not performed between samples of B sand.

The results of these comparisons (TABLE 1), indicate that significant differences occur predominantly at the higher order harmonics, 8, 9 and 10, with harmonic 10 displaying the greatest number of significant differences.

Two core locations, (1 and 8), are the farthest west in the sample array and are both almost due north of Bering Strait. The first orthogonal comparison compares these samples with the more landward samples, those at locations 2, 3, 4, 5, 9 and 12 (TABLE 3 and FIGURE 6). This comparison generated a significant difference at the second harmonic only, indicating that the seaward samples, 1 and 8, contained significantly greater numbers of more highly elongate grains. This suggests that Kobuk-Noatak sediment is present in significant amounts in the more shoreward samples, and that such sediment is significantly less highly elongate. This in turn suggests that the sum total of the diverse bottom current directions (FIGURES 4 and 5), have a strong northward component directly north of the Bering Strait, with a north westward component near shore.

All other significant differences in this hierarchy occur at the higher level harmonics, especially harmonic 10.

Of the two seaward locations, the northernmost, location 1, contains significantly less grains with a high tenth harmonic. There are two possible explanations for this.

First, as the A sand started its migration northward upon the opening of the Bering Strait, the current patterns were such as to allow for a higher degree of mixing in of Kobuk-Noatak type sediment with the more northerly of the Yukon sediment. This resulted in the northernmost location receiving a greater contribution of Kobuk-Noatak type sediment than did the more southerly sample. By the time the sediments were deposited at the southernmost location, the Kobuk-Noatak contribution was significantly diluted by the preponderance of Yukon sediments.

Secondly, the northernmost A sample, sample 1, must have passed through the strait considerably earlier than did the southernmost -- as much as several thousand years. A result of this time lag might be sediment of a significantly different character being transported at the leading edge of the wave front than that later derived sediment which followed.

The remaining orthogonal comparisons involve tests of hypotheses between the more shoreward samples. These samples display significant differences at harmonics 9 and 10. This variation was orthogonally partitioned in order to gain some insight into the pattern of diffusion.

The sample at location 12 is nearest the present Kobuk-Noatak delta, and was compared with the more northerly shoreward samples, 2, 3, 4, 5 and 9. No significant differences could be detected for harmonics 2-10, indicating either large scale homogeneity of shoreward samples, or that the more northern samples are different, but when summed resemble sample 12. Examination of the more northern samples indicates that differences do, in fact, exist between them (harmonics 8, 9 and 10).

Thus, location 12, although areally closest to the Kobuk-Noatak source, in terms of current pattern, (FIGURES 4 and 5), contains appreciably more Bering Strait sediment. That is, Kobuk-Noatak sediment may be transported predominantly north-westwardly along the coast, rather than due west through Kotzebue Sound.

This is supported by the results of comparisons between the remaining five shoreward samples (2, 3, 4, 5 and 9, excluding 12), which exhibits significant differences at harmonics 8, 9 and 10. This result, however, as can be seen in the next breakdown (A_9 versus $A_{2, 3, 4 \text{ and } 5}$), is generated solely by differences between the samples at locations 2, 3, 4 and 5, with location 9 not differing significantly from these except at the eighth harmonic. As with the comparison evaluating A_{12} versus $A_{2, 3, 4, 5, \text{ and } 9}$ the shape frequency distribution of the more southerly sample resembles that of the sum of the more northerly samples.

Hierarchy II

The second hierarchy, as previously discussed, involved harmonics 11 through 20, and was designed to evaluate variation within and between cores (TABLE 2).

The most striking result of this hierarchy was, even though the overall A vs. B contrast, as evaluated in hierarchy one, was non-significant, that there were significant differences between A and B sands in two cores. The A and B sands for PC090, location 2, differed significantly at harmonics 11 through 15, 17 and 18. Sample PC137, location 3, displayed a significant difference at harmonic 14.

This result supports the previous argument that the sands are constantly changing character, and that the non-significant overall A vs. B contrast was not a result of the sands being everywhere homogeneous.

Qualitatively, the remaining cores for which there was both an A and B sand range from A sands whose shape frequency distribution is essentially the same as B sands from other locations, to B sands whose shape frequency distribution is more A-like. (FIGURES 7, 8, 9, 10, 11, APPENDIX A).

This indicates that the processes involved in the sedimentation of the Chukchi Sea are not as simple as the tentative model proposed earlier, although in general, these results bear out the hypothesis.

The remainder of the second hierarchy concerned, primarily, differences between cores that had an A, but no B, and those that had a B, but no A. The results of these comparisons indicated a significant difference between the A sand at location 8 and that at location 12. This is, however, not to say that A_8 and A_{12} necessarily stem from a different source, but that there is a greater degree of mixing in of Kobuk-Noatak type material with the A sand at location 8 than with that at location 12, due to the pattern of current circulation.

This result amplifies the previous argument that location 12, although closest to the Kobuk-Noatak source, receives little contribution from that source, while an observable amount of mixing is taking place in the more seaward samples.

The comparison between unpaired B sands showed significant differences to exist between the B sands at locations 7, 10, and 11. It can be shown qualitatively, by inspection of the frequency distributions of these three samples, FIGURES 7, 8, 9, 10 and 11, that the difference is generated by a significant deficiency of grains having harmonic amplitude values in the higher ranges in sample 7.

These results indicate that the B sands, as the A, are changing character from location to location. This means that there must have been a significant amount of differential fluctuation in the provenance or the transport processes during the time of deposition of the B sands.

These fluctuations might be dependent upon a) particle size; b) environment of deposition, particularly whether the sediment was markedly wave reworked; c) distance of provenance.

CHAPTER V

CONCLUSIONS

The preceding analyses indicated that shape differences occur between sand samples from the Chukchi Sea. These differences are the manifestation of both stratigraphic and areal effects. That is, differences exist between some pairs of Recent A sands and the early Holocene B sands. Likewise, significant differences exist between A sands from location to location in the sample array, as well as between B sands.

In a technical sense, such results indicate presence of a location by strata interaction. This effect is undoubtedly the result of the complex transport and depositional history of the area.

The significant chi-square differences arise from changes in the polymodal shape frequency distributions from sample to sample (APPENDIX A). That significant differences are manifest principally at the higher order harmonics (e.g. 10-20), indicates that shape differences reside in the finer scaled shape characteristics. This suggests that grains in those samples characterized by low amplitudes for these harmonics may have been smoothed by abrasion or chemical etching. In that light such samples might represent grains that have passed through beach or littoral environments, whereas the grains with rougher surfaces may have been subjected to glacial-fluvial processes without subsequent beach abrasion.

Examination of the shape frequency data (APPENDIX A), indicates that most sands are represented by a dominant mode accompanied by lower valued peripheral modes. For the tenth harmonic, for instance, the amplitude frequency distribution generally displays a strong mode in the region .007 to .009. Samples A_2, A_8, B_3, and B_4, however, lack a dominant mode in this interval and in addition contain grains which are assigned to modes of considerably higher amplitude (to .014). The graphs for harmonics 14 and 18 exhibit shifts of the dominant mode to relatively higher values, or addition of higher valued modes.

Samples A_4, A_5, B_2, B_7, and B_{10} exhibit consistently lower values for harmonics 10, 14, and 18.

The rougher (those with high harmonic amplitudes) B sands occur in samples 3 and 4, northwest of Point Hope. The smoother samples may represent sands associated with estuarine beaches, whereas the locations containing the more angular material may represent fluvial sands that have bypassed this environment.

Smoother A sands occur west of Cape Dyer, whereas the rougher occur at location 8, directly north of the Bering Strait, and west of Cape Dyer. These latter samples contain a higher proportion of Yukon sediment, and the smoother, more Kobuk-Noatak.

These conclusions are at best tentative, due to the fact that they are based on such a small sample array.

At the least, however, the shape results indicate the presence of a complex pattern of shape variation in these sediments. Further resolution of that pattern should help delineate the sedimentary history of the region.

LIST OF REFERENCES

LIST OF REFERENCES

Ball, G. H., and Hall, D. J., 1967, A clustering technique for summarizing multivariate data: Behavioral Science, v.12, no. 2, pp. 153-155.

Creager, J. S., and McManus, D. A., 1965, Pleistocene drainage patterns on the floor of the Chukchi Sea: Marine Geology, v. 3, pp. 279-290.

__________, __________, 1967, Geology of the floor of Bering and Chukchi Seas--American Studies. The Bering Land Bridge (Symposium at the VII INQUA Congress) Stanford University Press, pp. 7-31.

Ehrlich, R., and Weinberg, B., 1970, An exact method for characterization of grain shape: Journal of Sedimentary Petrology, v. 40, no. 1, pp. 205-212.

Kimball, A. W., 1954, Short-cut formulas for the exact partition of χ^2 in contingency tables: Biometrics, v. X, pp. 452-458.

McManus, D. A., Echols, R. J., Creager, J. S., and Holmes, M. L., 1969, Holocene Oceanography of Chukchi Sea: American Assoc. Petroleum Geologists--Soc. Economic Paleontol. and Mineral. Annual Meeting, Dallas. (Abstract).

Orzeck, J., 1972, Fourier shape analysis of some beach, river and cliff sands from California [M.S. Thesis]: East Lansing, Michigan, Michigan State University.

Redmond, B., 1969, The utility of Fourier estimates of grain shape in sedimentological studies [M.S. Thesis]: East Lansing, Michigan, Michigan State University.

Waltz, S. R., 1972, Evaluation of shapes of quartz silt grains as provenance indicators in central Michigan [M.S. Thesis]: East Lansing, Michigan, Michigan State University.

APPENDICES

APPENDIX A

ISODATA CLUSTER CENTER ANALYSES

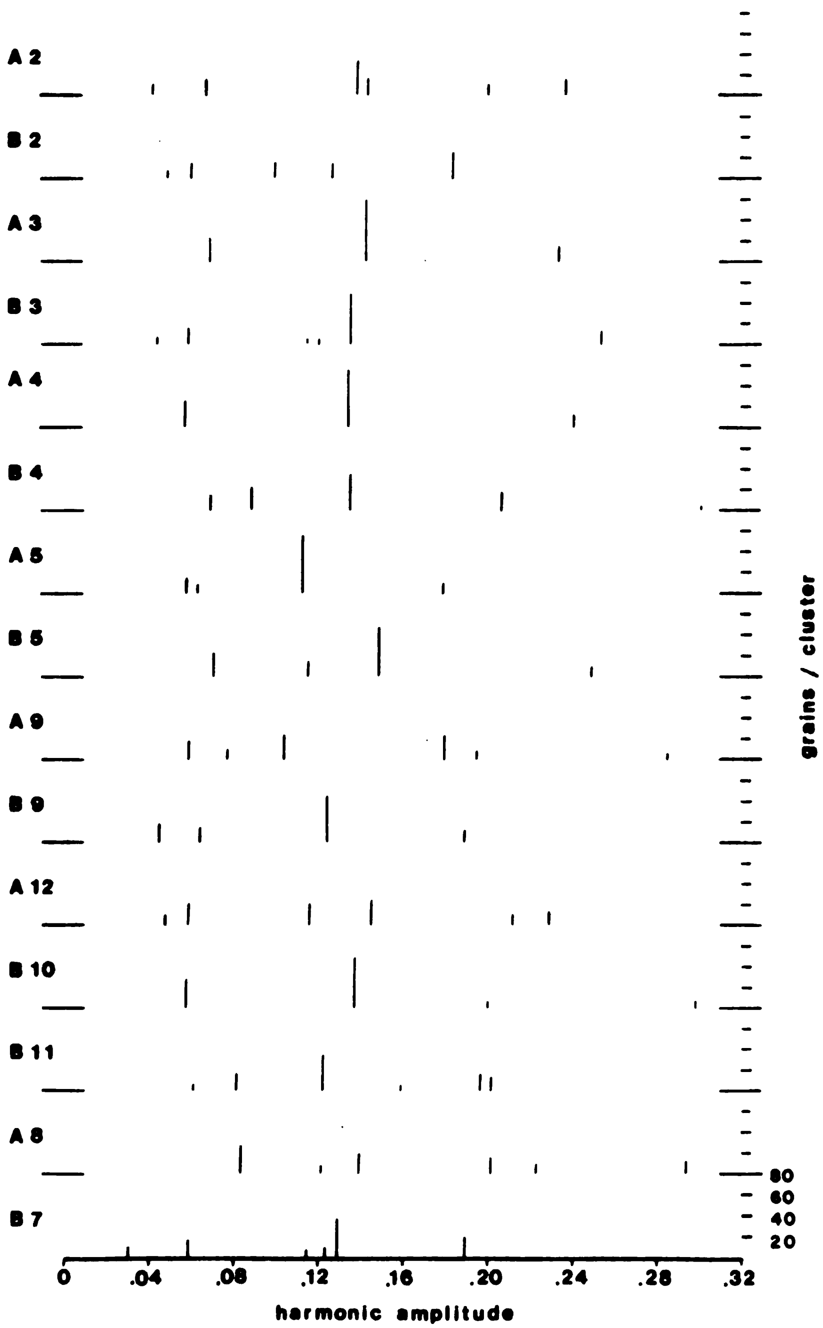

FIGURE 7.--ISODATA cluster center analysis (harmonic 2; all locations except location 1).

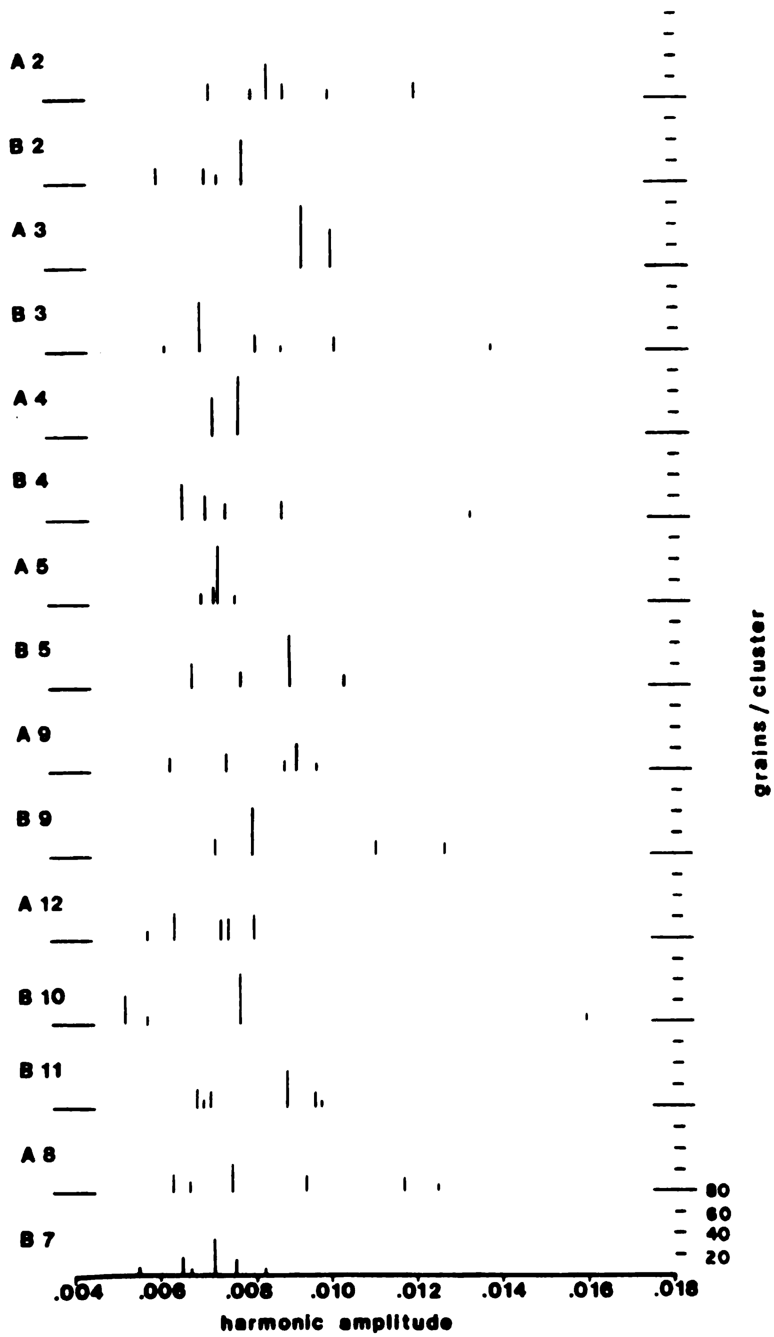

FIGURE 8.--ISODATA cluster center analysis (harmonic 10; all locations except location 1).

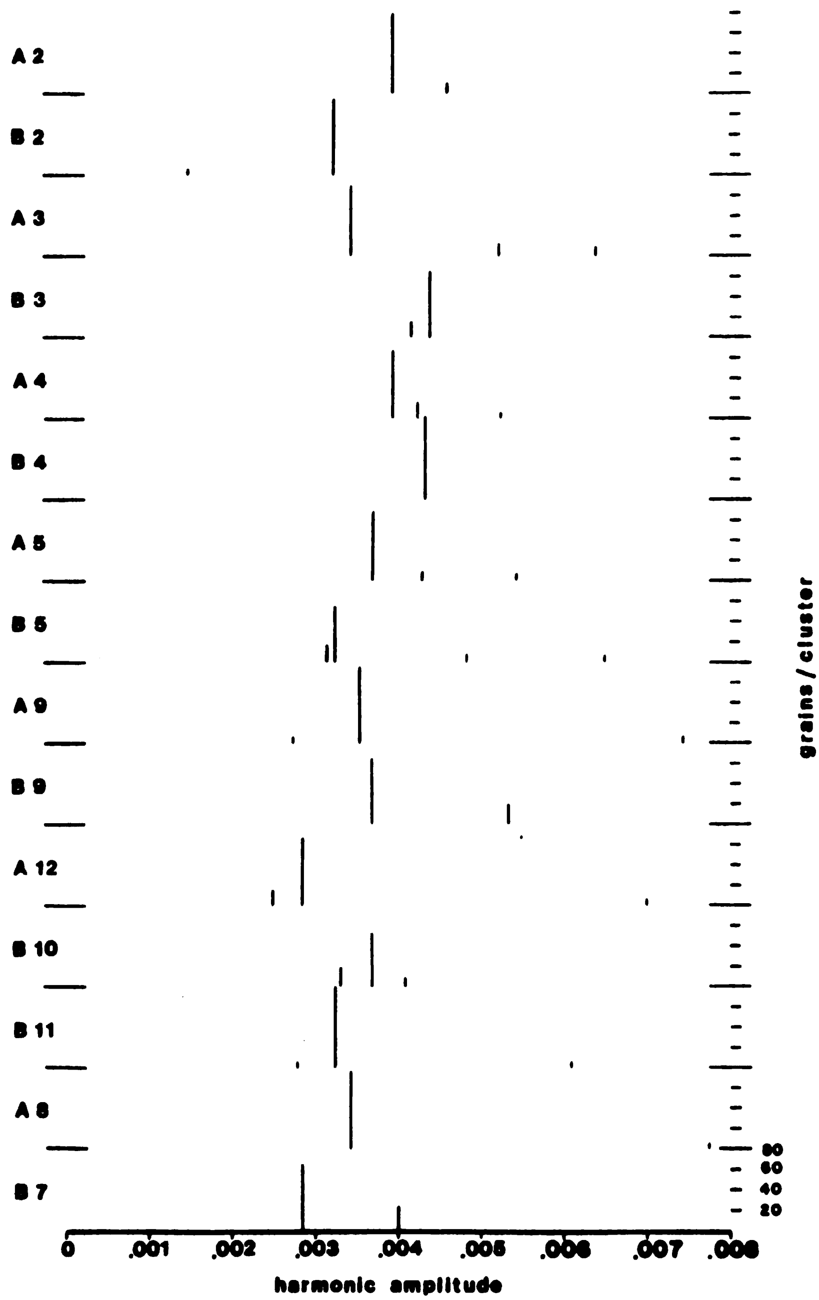

FIGURE 9.--ISODATA cluster center analysis (harmonic 14; all locations except location 1).

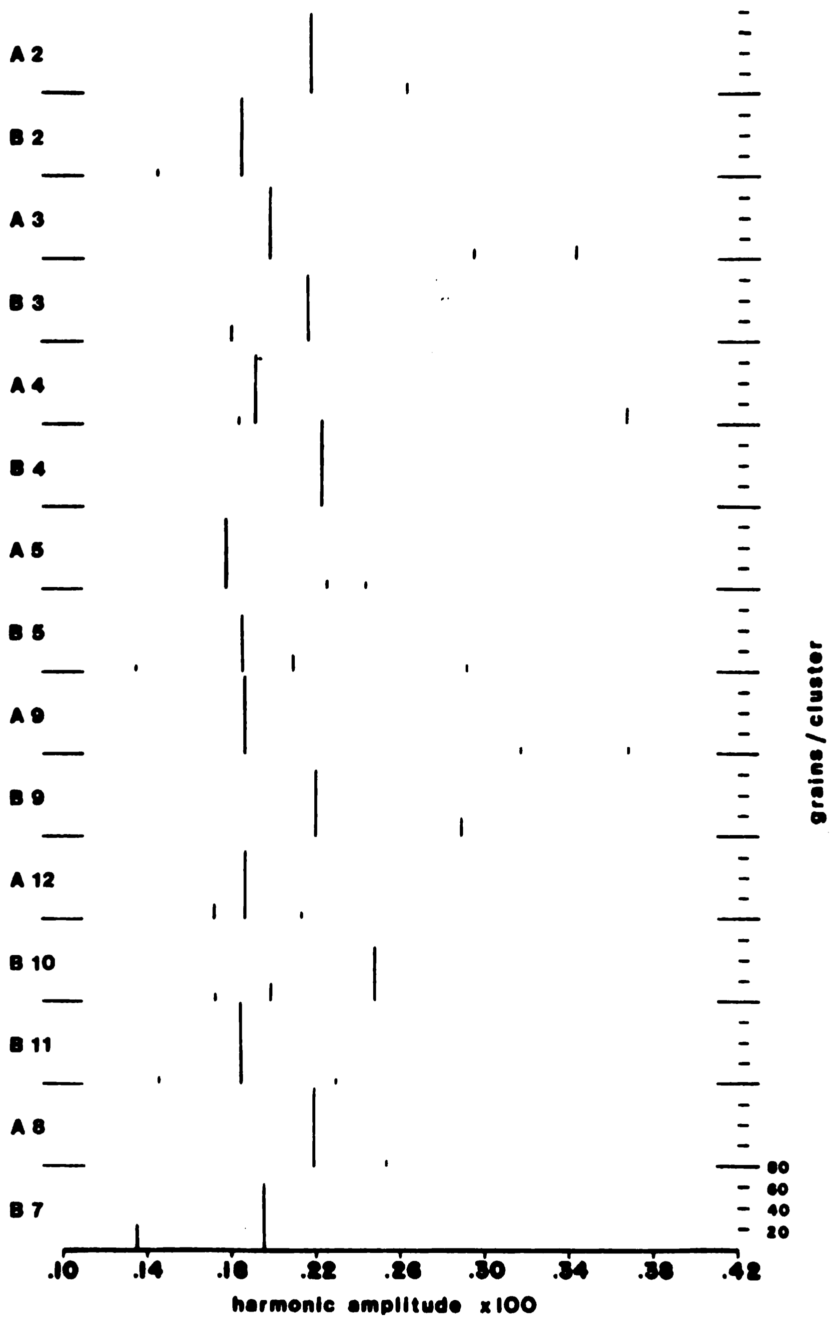

FIGURE 10.--ISODATA cluster center analysis (harmonic 18; all locations except location 1).

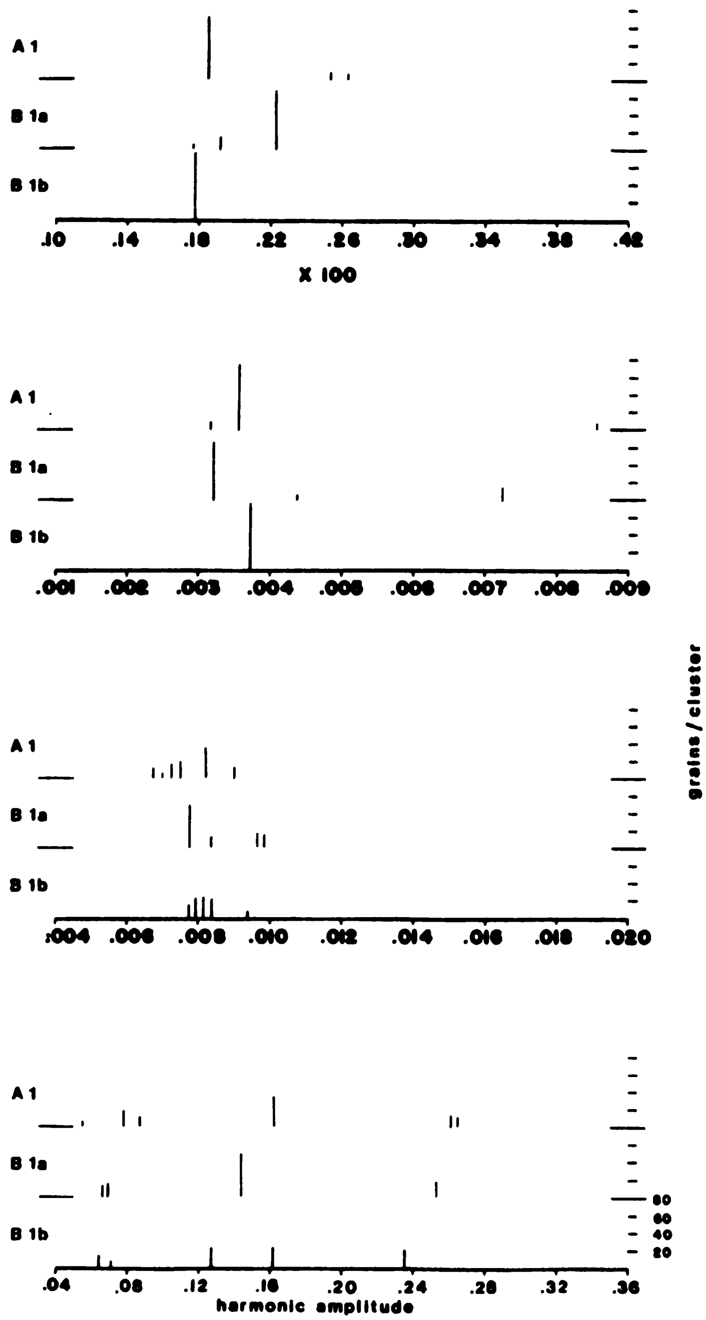

FIGURE 11.--ISODATA cluster center analysis for harmonics 2, 10, 14 and 18 at location 1.

APPENDIX B

NUMERICAL VALUES FOR CHI-SQUARE CONTINGENCY TABLES

TABLE 4.--Numerical values for chi-square contingency table (hierarchy I.)

Source of variability	d.f.	Harmonic 2	3	4	5	6	7	8	9	10
Total	85	109.9	80.7	101.3	72.7	102.4	67.7	94.2	112.4	116.1
A vs B	5	.9	6.9	9.5	10.0	10.0	3.0	5.6	9.2	5.4
Within A vs B	80	107.0	73.8	91.8	62.7	92.4	64.6	88.5	103.2	110.7
Between A	35	47.7	37.4	42.4	26.4	39.7	20.3	44.4	46.5	60.4
$A_{+3+4+5+}$ $9+12$ vs A_1+A_8	5	19.7	.7	7.4	4.9	5.4	3.9	5.1	3.5	5.6
A_{1+8}vs A_2 vs3vs4vs5 vs9vs12	30	28.0	36.7	35.3	21.4	34.4	16.4	39.3	43.0	54.7
A_1 vs A_8	5	2.5	1.5	4.9	1.7	4.3	2.0	3.0	5.2	12.1
Between $A_{2,3,4,5,}$ $9,12$	25	25.6	35.2	30.4	19.7	30.1	14.5	36.3	37.8	42.6
A_{12} vs A_{2+} $3+4+5+9$	5	1.2	5.5	3.1	4.3	8.3	4.4	2.3	5.8	7.8
Between $A_{2,3,4,5,9}$	20	24.4	30.0	27.3	15.4	21.7	10.1	34.0	32.0	34.9
A_9 vs A_{2+3} $+4+5$	5	7.6	7.0	8.3	2.2	2.4	1.8	14.7	4.4	2.7
Between $A_{2,3,4,5}$	15	16.8	23.0	19.0	13.2	19.3	8.3	19.3	27.5	32.1
Between B	45	59.3	36.3	49.1	36.3	52.7	44.3	44.1	56.7	50.3

* For significant harmonics, see TABLE 1.

TABLE 5.--Results of contingency tables (hierarchy II.)

Source of variability	d.f.	Harmonic 11	12	13	14	15	16	17	18	19	20
Total	80	85.3	93.3	111.7	114.9	101.9	107.6	107.0	107.5	89.8	101.3
Between cores	25	23.3	29.8	20.6	30.4	27.4	32.7	32.9	27.6	31.7	39.5
Bet.AvsB W/cores	30	38.2	43.0	55.2	42.7	36.0	35.9	32.5	36.9	32.5	17.2
A_1 vs B_1	5	4.3	3.4	1.9	8.7	1.4	7.0	3.5	4.2	2.0	3.5
A_2 vs B_2	5	18.5	17.2	32.8	11.5	14.5	9.2	17.3	14.7	3.3	4.4
A_3 vs B_3	5	2.8	4.7	5.3	12.1	7.3	3.6	1.9	1.8	9.7	2.3
A_4 vs B_4	5	5.3	6.9	2.0	6.6	7.5	9.6	1.9	5.6	5.7	.5
A_5 vs B_5	5	4.7	6.4	4.3	.8	2.8	2.0	6.5	1.7	4.4	3.9
A_9 vs B_9	5	2.5	4.4	8.9	3.1	2.5	4.5	1.4	8.8	7.3	2.5
Tot. bet unpaired A and B	20	13.6	25.4	21.3	25.9	28.5	25.4	33.4	36.9	24.4	33.0
A_8 vs A_{12}	5	3.2	5.6	3.7	9.0	9.4	14.1	9.3	9.4	9.3	8.6
B_7 vs B_{10} vs B_{11}	10	7.0	19.1	12.5	10.7	14.3	13.9	14.0	24.4	12.9	16.5
A_8+A_{12} vs B_7+B_{10}+B_{11}	5	3.3	.7	5.1	6.2	4.8	7.4	10.1	3.2	2.1	7.9

* For significant harmonics, see TABLE 2.

APPENDIX C

LOCALITY MAPS

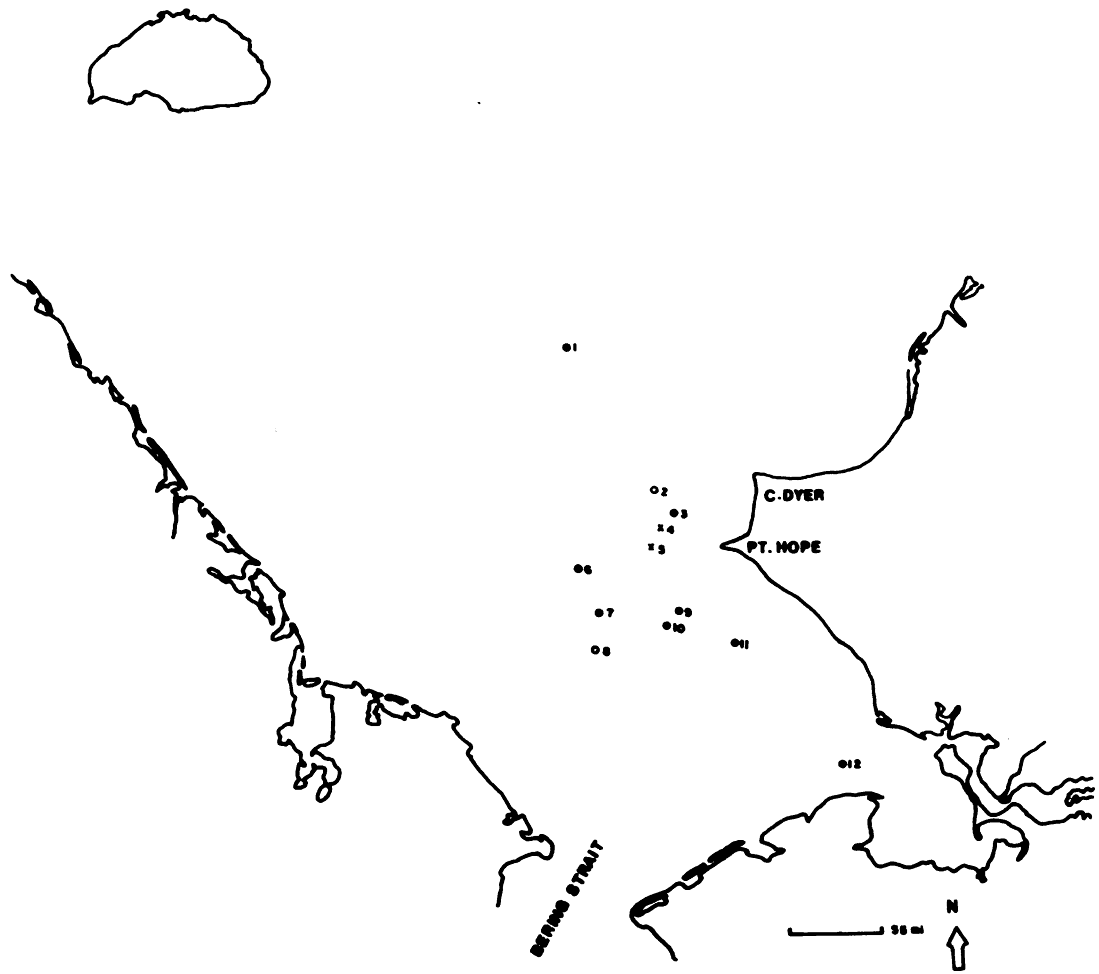

FIGURE 12.--Map showing locations of most rounded (x) and most angular (o) A sands.

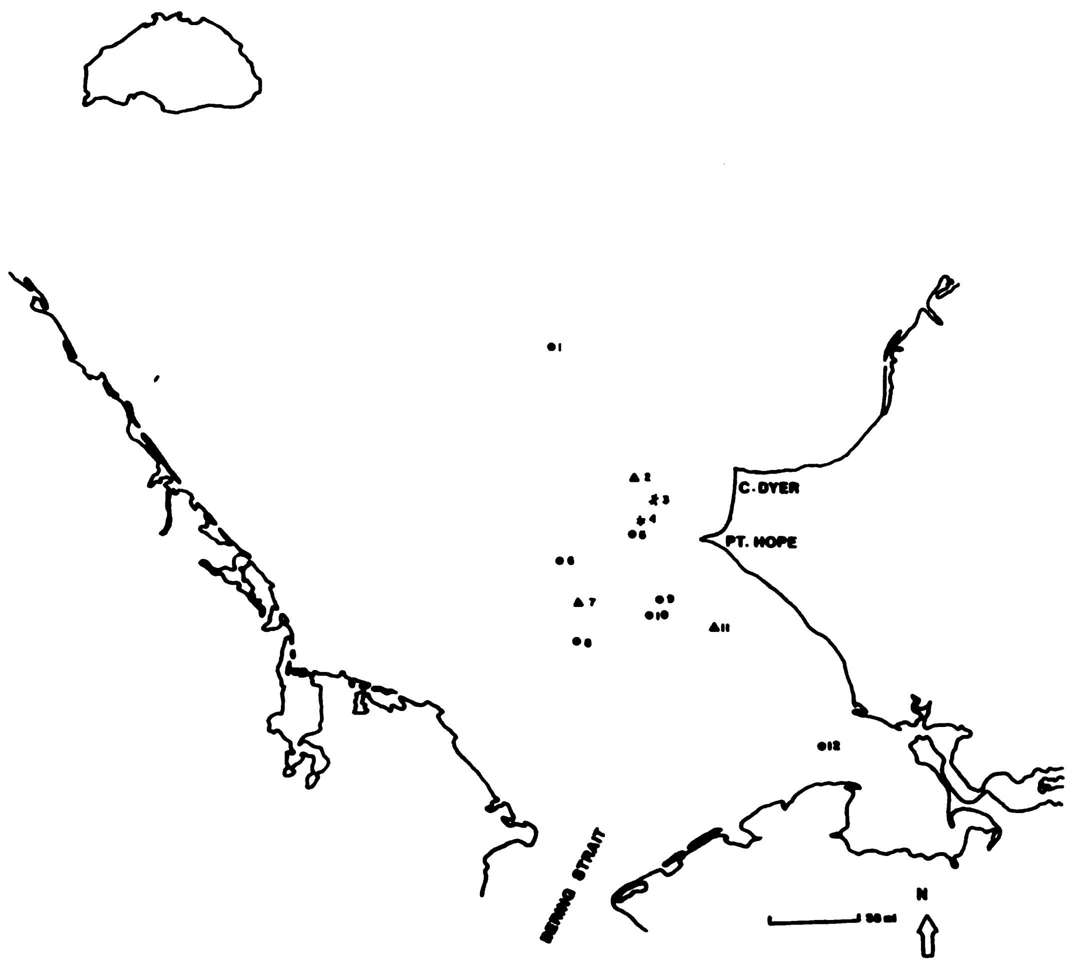

FIGURE 13.--Map showing locations of most rounded (▲) and most angular (*) B sands.